^{18}F-FDG and ^{18}F-FET uptake in experimental soft tissue infection

Achim H. Kaim[1], Bruno Weber[1], Michael O. Kurrer[2], Gerrit Westera[3], Alain Schweitzer[4], Jochen Gottschalk[5], Gustav K. von Schulthess[1], Alfred Buck[1]

[1] Nuclear Medicine, University Hospital Zurich, Rämistrasse 100, 8091 Zurich, Switzerland
[2] Department of Pathology, University Hospital Zurich, Switzerland
[3] Center for Radiopharmaceutical Sciences, University Hospital Zürich, Switzerland
[4] Novartis Pharma Inc, Basel, Switzerland
[5] Institute of Medical Microbiology, University Hospital Zurich, Switzerland

Received 24 November 2001 and in revised form 27 January 2002 / Published online: 6 March 2002

Abstract. The aim of this study was to compare the uptake of ^{18}F-fluoroethyl-L-tyrosine (^{18}F-FET) with that of ^{18}F-fluorodeoxyglucose (^{18}F-FDG) in activated inflammatory white blood cells. Unilateral thigh muscle abscesses were induced in 11 rats by intramuscular inoculation of 0.1 ml of a bacterial suspension (*S. aureus*, 1.2×10^9 CFU/ml). Four animals were intraperitoneally injected with 130–180 MBq ^{18}F-FDG, four with 140–170 MBq ^{18}F-FET and three with a mixture of 140–170 MBq ^{18}F-FET and 1.8 MBq ^{14}C-deoxyglucose. Autoradiography (10 µm slice thickness) of the abscess and the contralateral muscle was performed and detailed spatial correlation of autoradiography and histopathology (haematoxylin-eosin staining) was obtained. Regions of interest were placed on the abscess wall and the grey values (digitised image intensities) measured were converted to kBq/cc per kBq injected activity per gram (SUV). Areas with increased ^{18}F-FDG uptake corresponded to cellular inflammatory infiltrates mainly consisting of granulocytes. The SUV was calculated to be 4.08±0.65 (mean±SD). The uptake of ^{18}F-FET in activated white blood cells was not increased: the SUV of the abscess wall, at 0.74±0.14, was even below that of contralateral muscle. The low uptake of ^{18}F-FET in non-neoplastic inflammatory cells promises a higher specificity for the detection of tumour cells than is achieved with ^{18}F-FDG, since the immunological host response will not be labelled and inflammation can be excluded.

Keywords: Soft tissue infection – Fluorine-18 fluorodeoxyglucose – Autoradiography – Fluorine-18 fluoroethyl-L-tyrosine

Achim H. Kaim (✉)
Nuclear Medicine, University Hospital Zurich, Rämistrasse 100, 8091 Zurich, Switzerland
e-mail: Achim.Kaim@dmr.usz.ch
Tel.: +41-1-2553404, Fax: +41-1-2554428

Eur J Nucl Med (2002) 29:648–654
DOI 10.1007/s00259-002-0780-y

Introduction

Radiolabelled amino acids have proven to be useful for imaging in clinical oncology, especially for brain tumours [1, 2], lymphoma [3], lung [4] and breast cancer [5]. The tumour uptake is thought to reflect increased amino acid metabolism of cancer cells, such as increased active transport and protein synthesis. Carbon-11 labelled amino acids are suitable for positron emission tomography (PET) imaging, but because of the short half-life of ^{11}C ($t_{1/2}$=20 min), the availability of these tracers is limited to PET centres with an in-house cyclotron, preventing their widespread use. Recently, the synthesis and use of a fluorine-18 labelled amino acid, ^{18}F-fluoroethyl-L-tyrosine (^{18}F-FET), has been reported [2]. ^{18}F-FET has the advantages of a longer half-life ($t_{1/2}$=110 min) and a simple and efficient synthesis. The physical properties of this tracer are suitable for the acquisition of whole-body PET scans, and it seems promising for use in clinical oncology. ^{18}F-FET is an analogue of tyrosine that is not metabolised and not incorporated into proteins but is actively transported into tumour cells. The synthetic yields are higher than with another recently published ^{18}F-labelled tyrosine, ^{18}F-fluoro-α-methyl tyrosine (^{18}F-FMT) [6], and are sufficient for satellite distribution. In accordance with findings obtained with other radiolabelled amino acids [7, 8], first clinical experience with ^{18}F-FMT suggests that it is not significantly incorporated into inflammatory cells [9]. Assuming a similar effect for ^{18}F-FET, a more tumour-specific uptake can be expected in comparison with ^{18}F-fluorodeoxyglucose (^{18}F-FDG), the uptake of which reflects not only accumulation in cancer cells but also the tumour-

host immune system reaction [10, 11]. Moreover, ^{18}FET-PET might assist in the differentiation of infection and recurrent tumour, which is occasionally difficult in the follow-up during tumour treatment with ^{18}F-FDG. Thus it is of major interest to evaluate whether there is ^{18}F-FET uptake in inflammation in order to determine its specific value in clinical PET imaging.

The purpose of this study was to investigate ^{18}F-FET uptake in activated inflammatory cells using an experimental acute abscess model and semiquantitative autoradiography, and to compare it with ^{18}F-FDG accumulation. In a second step, we correlated the tissue distribution of ^{18}F-FET with that of ^{14}C-deoxyglucose (^{14}C-DG) by means of a dual-tracer autoradiography experiment.

Materials and methods

Animals and abscess model. The study was performed according to the guidelines of the National Institutes of Health and the recommendations of the committee on animal research at our institution. The protocol was fully approved by the local institutional review committee on animal care.

The study included 11 OFA rats (stock IcoIbm: OFA) (weight 250–300 g). All the animals were kept in cages with standardised conditions of light and free access to water and food. Using general inhalation anaesthesia (methoxyfluranum, Pitman-Moore Inc., USA), left-sided, a unilateral deep calf muscle abscess was induced by intramuscular inoculation (25G needle) of 0.1 ml of a bacterial suspension (*S. aureus*, clinical strain 10B, Novartis Pharma, Inc., Switzerland). One author measured bacterial concentration (1.2×10^9 CFU/ml) by optical density (McFarland Standard, bioMerieux, Inc., USA).

All animals developed a palpable fluctuating mass in the left calf muscle within 36 h after bacterial inoculation. No systemic infection occurred.

Autoradiography with ^{18}F-FDG. Four rats bearing an abscess (48 h after bacterial inoculation) in the left calf muscle were intraperitoneally injected with a dose of 130–180 MBq ^{18}F-FDG and sacrificed 45 min later by an intracardiac overdose of pentobarbital. Infected calf muscle and contralateral normal calf muscle were dissected immediately and frozen in isopentane cooled to –50ºC. The frozen samples were cut (10 µm thickness) and thaw-mounted on glass slides. Film (Biomax MR, Kodak, USA) was subsequently exposed for 24 h together with ^{14}C standards for later quantification of grey values (digitised image intensities). The slices were then stained using haematoxylin-eosin (HE) for histological examination.

Autoradiography with ^{18}F-FET. Another four rats bearing an abscess (48 h after bacterial inoculation) in the left calf muscle were intraperitoneally injected with a dose of 140–170 MBq ^{18}F-FET and sacrificed 45 min later by an intracardiac overdose of pentobarbital. Animal preparation, tissue sampling, autoradiographic technique and staining were as described in the previous section.

Dual-tracer autoradiography. Three rats bearing an abscess (48 h after bacterial inoculation) were intraperitoneally injected with a mixture of 140–170 MBq ^{18}F-FET and 1.8 MBq ^{14}C-DG dissolved in 3 ml saline and sacrificed 45 min later by an intracardiac overdose of pentobarbital. Infected calf muscle and the contralateral normal calf muscle were dissected immediately and frozen in isopentane cooled to –50ºC. The frozen samples were cut (10 µm thickness) and thaw-mounted on glass slides. A phosphor imaging plate (BAS-TR2025, Fuji Photo Film Co., Japan) was subsequently exposed for 4 h to produce ^{18}F-FET images. Three days later the sections with residual ^{14}C-DG activity were placed in contact with a separate phosphor imaging plate for 7 days. The slices were then stained using HE for histological examination.

Quantitative analysis. In a calibration experiment, each ^{14}C standard was assigned a value in kBq/cc of ^{18}F activity. For this purpose, 10-µm-thick slices of a brain paste that contained defined amounts of ^{18}F activity (kBq/mg) were exposed on film together with the ^{14}C standard for 24 h.

Autoradiographs were digitised and the grey values converted to kBq/mg using the calibrated ^{14}C standards. The activities were then decay corrected to the time of injection. Dividing these values by the amount of injected activity per gram of body weight yielded standardised uptake values (SUVs). On ^{18}F-FDG and ^{18}F-FET digitised autoradiographs, regions of interest (ROIs) were placed on the abscess wall and contralateral muscle and the SUVs were calculated. To define the exact site of the ROIs, stained histological sections were considered. The size of the ROIs was adjusted to the individual abscess configuration (range 0.011–0.056 cm^2).

A Wilcoxon rank sum test was performed comparing the medians of the differences between the SUV of the abscess wall and the SUV of the contralateral muscle for ^{18}F-FET and ^{18}F-FDG.

Qualitative analysis. Detailed histomorphological comparison between histology and autoradiography was performed. Both autoradiographs and histological specimens were digitised and image fusion allowed optimal spatial correlation. The ^{18}F-FET, ^{18}F-FDG or ^{14}C-DG uptake was assigned to inflammatory cell infiltration, tissue necrosis and muscle on histopathology. The cells of the inflammatory infiltration were histologically characterised as neutrophil granulocytes, macrophages or lymphocytes.

Results

Histomorphological correlation to ^{18}F-FDG autoradiography

The acute abscess formation was histologically characterised by central necrosis predominantly surrounded by neutrophils, and to a lesser degree by macrophages. A second necrotic tissue layer was delineated between the inner granulocyte layer and a more peripherally localised cellular infiltration that consisted mainly of granulocytes and some interspersed macrophages. The areas with increased ^{18}F-FDG uptake corresponded to cellular inflammatory infiltrates mainly consisting of granulocytes. The necrotic abscess centre and the second necrotic tissue layer were characterised by decreased ^{18}F-FDG uptake. The SUVs (mean±SD) of the inner and outer cellular zones were 4.08±0.65 and 3.11±0.52, respectively. Figure 1 shows a typical autoradiograph with corresponding histology.

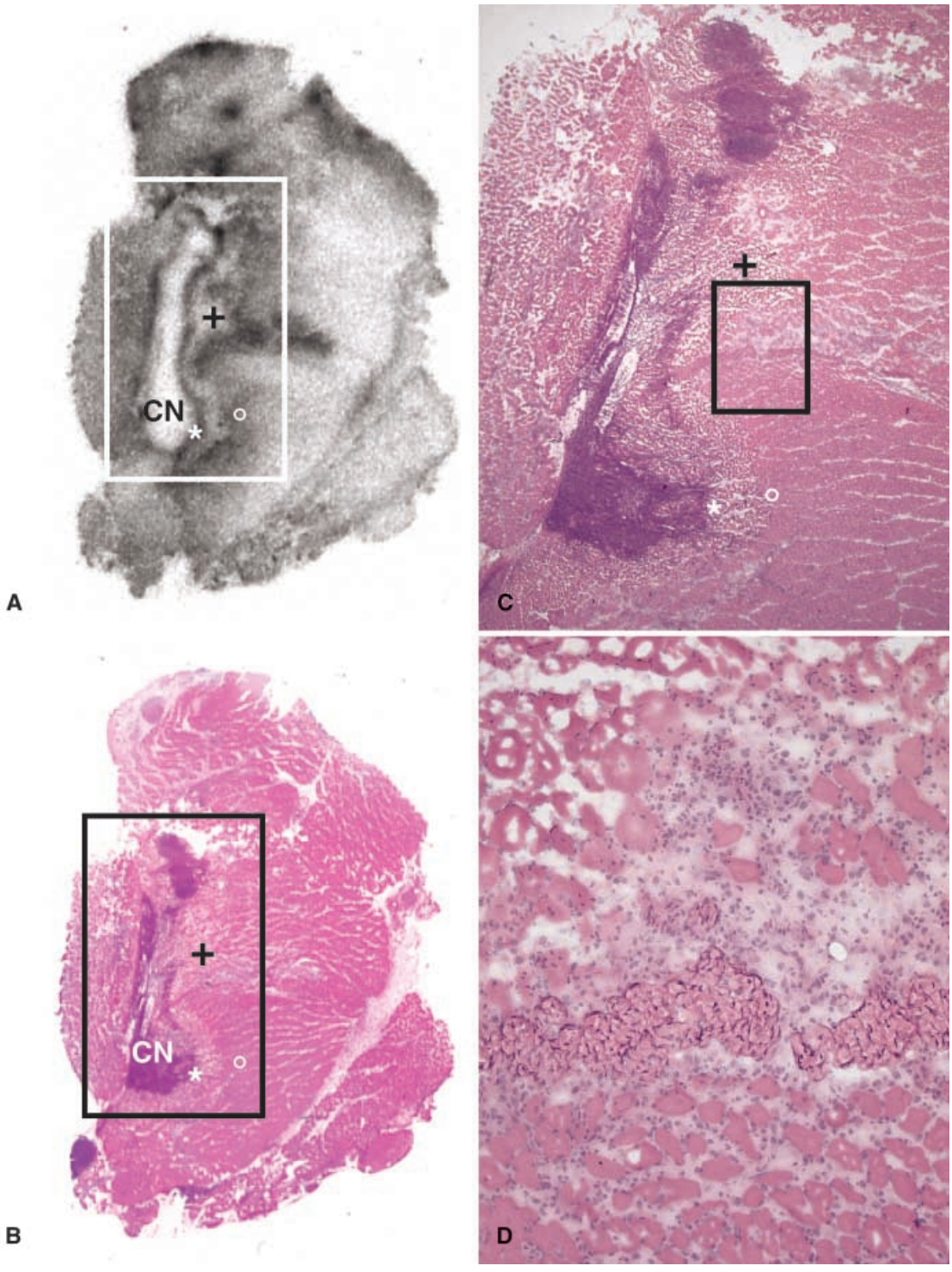

Fig. 1. ^{18}F-FDG autoradiograph (**A**), corresponding section (HE) (**B**) and histology (**C** ×1.25, **D** ×10) of an acute intramuscular abscess. The abscess is characterised by central necrosis (*CN*), an inner layer of inflammatory cells mainly consisting of granulocytes (*white star*), a second necrotic muscle layer (*black cross*) and an outer layer (*white circle*) of predominantly granulocytes. Areas with increased ^{18}F-FDG accumulation correspond to cellular infiltrates (**D**)

Histomorphological correlation to ^{18}F-FET autoradiography

The areas with inflammatory cell infiltrates consisting mainly of granulocytes and some macrophages did not exhibit increased uptake of ^{18}F-FET in comparison with the surrounding muscle. Differentiation of the inner and outer cellular zones was not possible on autoradiographs. The necrotic abscess centre could be identified by virtue

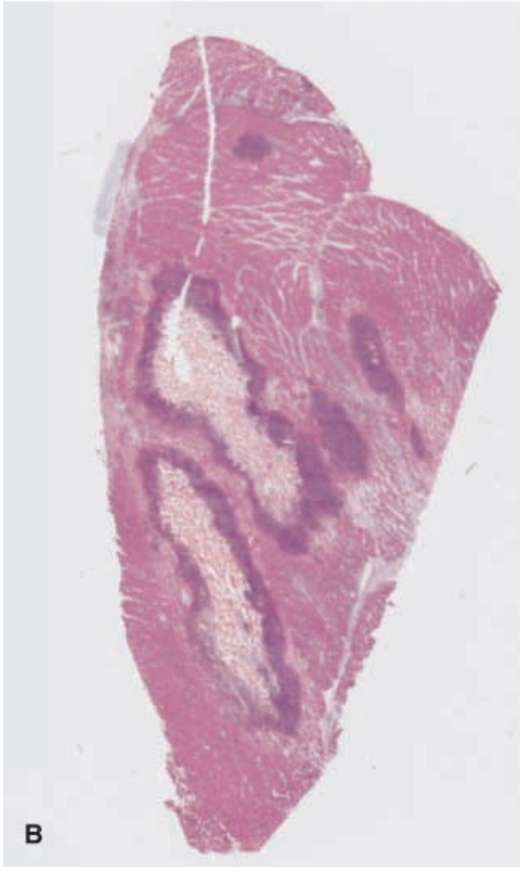

of decreased ^{18}F-FET accumulation. The ROI of the inner layer corresponding to the abscess wall close to the central necrosis was placed with reference to the histological slices in order to ensure measurement at the correct site. The SUV was calculated to be 0.74±0.14 and was even less than the SUV of the contralateral muscle (1.28±0.19). Figure 2 shows a typical autoradiograph with corresponding histology.

Dual-tracer autoradiography

Figure 3 shows typical autoradiographs of an abscess after injection of a mixture of ^{18}F-FET and ^{14}C-DG. The ^{14}C-DG autoradiographs were more heterogeneous owing to the intense uptake of the tracer into the activated white blood cells. The areas of ^{14}C-DG accumulation could be assigned to granulocytes and macrophages. The visual contrast on ^{18}F-FET autoradiographs was very low since the accumulation of the radiolabelled amino acid in the surrounding muscle and the inflammatory cells was quite similar. Areas of increased ^{14}C-DG accumulation did not exhibit similar intense radioactivity with ^{18}F-FET.

Statistical analysis

The SUVs are illustrated in Fig. 4. The median of the differences between the SUV of the abscess wall and the SUV of contralateral muscle was significantly greater for ^{18}F-FDG than for ^{18}F-FET ($P<0.05$, two-tailed).

Discussion

The clinical application of radiolabelled amino acids has been severely limited by the lack of a tracer that is as widely available as ^{18}F-FDG. The fluorine label with a half-life of 110 min and the short, high-yield radiosynthesis of ^{18}F-FET meet the requirements for routine widespread clinical application. The amino acid transport is the dominant step in the increased tracer accumulation in tumour cells [12], and the tracer is not metabolised and incorporated into proteins. First clinical studies have demonstrated the usefulness of ^{18}F-FET scan in patients with primary brain tumours and metastasis, the uptake pattern and imaging contrast being similar to those observed with ^{11}C-methionine [2]. Experimental studies in tumour-bearing mice have shown a high accumulation

◀ **Fig. 2.** ^{18}F-FET autoradiograph (**A**) and corresponding section (HE) (**B**) of an acute intramuscular abscess. The areas with inflammatory cell infiltrates consisting mainly of granulocytes and some macrophages did not show an increased uptake of ^{18}F-FET in comparison with the surrounding muscle

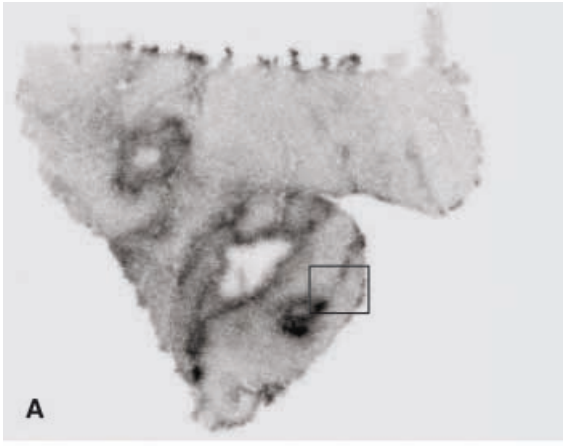

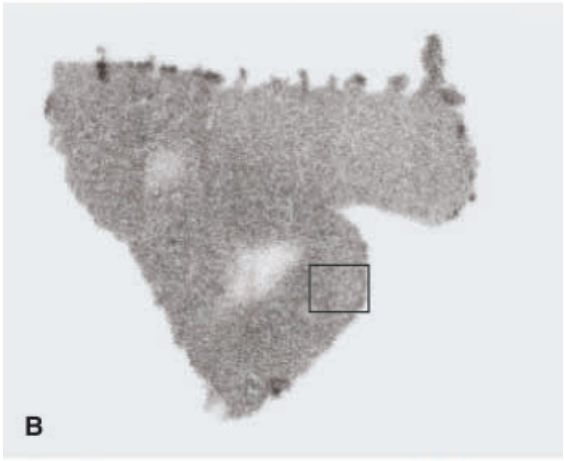

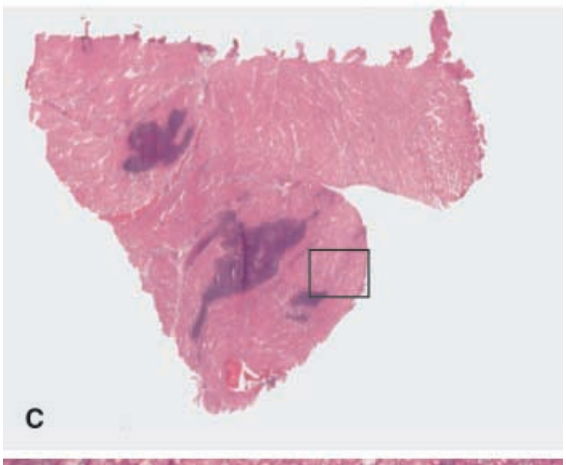

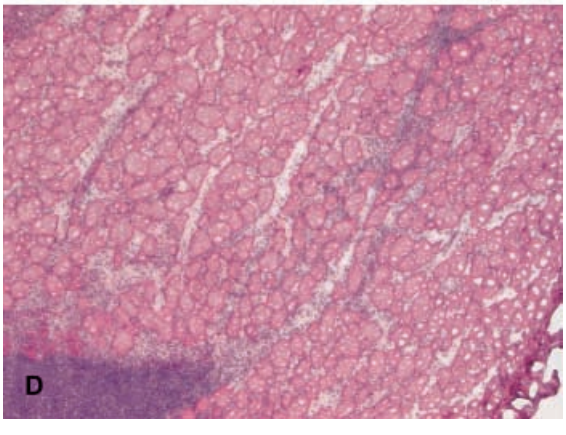

◀ **Fig. 3.** Dual-tracer autoradiography (**A, B**) and corresponding section (HE) (**C**) and histology (**D**, ×5) of an acute abscess. ^{14}C-DG autoradiography (**A**) demonstrates increased tracer activity in the abscess wall which can be assigned to inflammatory cells (**C, D**). The same areas do not exhibit increased accumulation on ^{18}F-FET autoradiography (**B**) in comparison with the surrounding muscle tissue

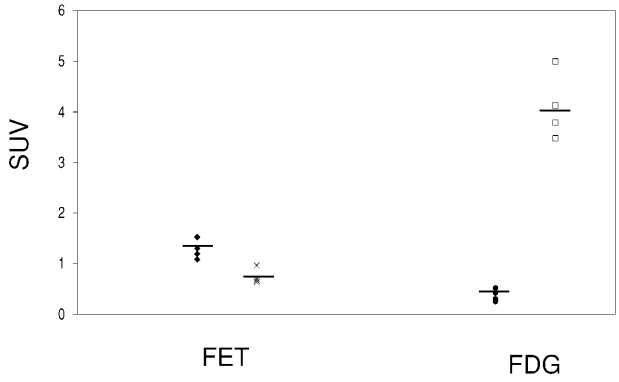

Fig. 4. SUVs (individual values) of the abscess wall and contralateral muscle on ^{18}F-FET and ^{18}F-FET autoradiographs (*black rhombus*, SUV_{FET} contralateral muscle; *cross*, SUV_{FET} abscess wall; *black circle*, SUV_{FDG} contralateral muscle, *white square*, SUV_{FDG} abscess wall)

of ^{18}F-FET in colon and mammary carcinoma similar to the results with other artificial amino acids [13], which reflects the hypermetabolic state of viable tumour cells. Since previous findings with other radiolabelled amino acids have not shown evidence of tracer uptake into inflammatory cells, ^{18}F-FET is a very promising substance for oncology, and potentially more specific than ^{18}F-FDG. To investigate selectively the uptake of ^{18}F-FDG and ^{18}F-FET into activated inflammatory cells, we used a physiological, bacterial soft tissue abscess model and autoradiography, which enabled us to perform histomorphological correlation and calculation of SUVs in different areas.

Upon exposure to certain stimuli, including infection, ischaemia, tumours, trauma or foreign bodies, phagocytes (both neutrophils and macrophages) start metabolising large quantities of glucose by way of the hexose monophosphate shunt, and their rates of oxygen uptake increase greatly, sometimes more than 50-fold [14]. This transformation of the resting cells into activated phagocytes is known as “respiratory burst”. Energy-dependent, interrelated cellular defence mechanisms include migration, generation and release of microbicidal agents and phagocytosis [15, 16]. In agreement with previous clinical and experimental studies [17, 18, 19, 20, 21, 22], we documented a marked increase in ^{18}F-FDG uptake at the site of infection, which could be assigned to activated granulocytes and macrophages. The

transporter activity of ^{18}F-FET, however, was not affected by the hypermetabolic state of activated cells and did not lead to an increased uptake into white blood cells. The consumption of amino acids is evidently not influenced by various intracellular pathways, including stimulus-induced increases in the phospholipid mechanism of cell membranes and protein kinase C activation [23]. The accumulation of ^{18}F-FET and ^{18}F-FDG in activated inflammatory cells was quantitatively assessed by ^{18}F-FET and ^{18}F-FDG autoradiography. In the case of ^{18}F-FET, the SUV in areas of inflammatory infiltration was even below that in contralateral muscle. The dual-tracer experiment with ^{18}F-FET and ^{14}C-DG permitted exact morphological correlation between areas of increased deoxyglucose uptake due to activated cells and ^{18}F-FET accumulation and did not reveal elevated ^{18}F-FET radioactivity.

The bacterial consumption of ^{18}F-FDG or ^{18}F-FET could not be discriminated from cellular uptake, although it is known that abscess-forming bacteria utilise glucose as an energy source and may accumulate amino acids [24]. The problems were the mixed pattern of inflammatory cells and bacteria and the small bacterial size, which could not be resolved with the applied technique. However, the low accumulation of ^{18}F-FET in areas where presence of bacteria is expected may be explained by either lacking bacterial ^{18}F-FET uptake or a low bacterial density.

Experimental and clinical findings have documented that ^{18}F-FET accumulates in tumours with a high affinity. Our study showed that ^{18}F-FET uptake is low in inflammatory infiltrates consisting of neutrophil granulocytes and macrophages. This suggests that ^{18}F-FET allows the clear differentiation of neoplasms and acute inflammatory lesions, which is equivalent to offering improved specificity in tumour diagnosis. With regard to tumour therapy monitoring, it may be relevant whether the tumour-associated inflammatory response accumulates ^{18}F-FET. This cannot be definitively excluded on the basis of our study since the composition of inflammatory cells involved in the immune response to tumours is somewhat different from that observed in acute infection and mainly consists of T-lymphocytes and macrophages. Further clinical studies are required to prove that tumour detection with ^{18}F-FET is at least as sensitive as with ^{18}F-FDG.

Acknowledgements. The authors would like to thank Mr Tibor Cservenyak of the cyclotron unit for his excellent technical assistance.

This work was supported by Novartis-Stiftung Basle, Switzerland, EMDO-Stiftung Zurich, Switzerland and Freie Akademische Gesellschaft, (FAG) Basle, Switzerland.

References

1. Langen KJ, Ziemons K, Kiwit JC, et al. 3-[^{123}I]iodo-alpha-methyltyrosine and [methyl-^{11}C]-L-methionine uptake in cerebral gliomas: a comparative study using SPECT and PET. *J Nucl Med* 1997; 38:517–522.
2. Weber WA, Wester HJ, Grosu AL, et al. *O*-(2-[^{18}F]fluoroethyl)-L-tyrosine and L-[methyl-^{11}C]methionine uptake in brain tumours: initial results of a comparative study. *Eur J Nucl Med* 2000; 27:542–549.
3. Leskinen Kallio S, Ruotsalainen U, Nagren K, Teras M, Joensuu H. Uptake of carbon-11-methionine and fluorodeoxyglucose in non-Hodgkin's lymphoma: a PET study. *J Nucl Med* 1991; 32:1211–1218.
4. Nettelbladt OS, Sundin AE, Valind SO, et al. Combined fluorine-18-FDG and carbon-11-methionine PET for diagnosis of tumors in lung and mediastinum. *J Nucl Med* 1998; 39:640–647.
5. Leskinen Kallio S, Nagren K, Lehikoinen P, Ruotsalainen U, Joensuu H. Uptake of ^{11}C-methionine in breast cancer studied by PET. An association with the size of S-phase fraction. *Br J Cancer* 1991; 64:1121–1124.
6. Inoue T, Tomiyoshi K, Higuichi T, et al. Biodistribution studies on L-3-[fluorine-18]fluoro-alpha-methyl tyrosine: a potential tumor-detecting agent. *J Nucl Med* 1998; 39:663–667.
7. Kubota R, Kubota K, Yamada S, et al. Methionine uptake by tumor tissue: a microautoradiographic comparison with FDG. *J Nucl Med* 1995; 36:484–492.
8. Kubota K, Ishiwata K, Kubota R, et al. Feasibility of fluorine-18-fluorophenylalanine for tumor imaging compared with carbon-11-L-methionine. *J Nucl Med* 1996; 7:320–32
9. Inoue T, Koyama K, Oriuchi N,et al. Detection of malignant tumors: whole-body PET with fluorine 18 alpha-methyl tyrosine versus FDG-preliminary study. *Radiology* 2001; 220:54–62.
10. Kubota K, Kubota R, Yamada S. FDG accumulation in tumor tissue. *J Nucl Med* 1993; 34:419–421.
11. Kubota R, Yamada S, Kubota K, Ishiwata K, Tamahashi N, Ido T. Intratumoral distribution of fluorine-18-fluorodeoxyglucose in vivo: high accumulation in macrophages and granulation tissues studied by microautoradiography. *J Nucl Med* 1992; 33:1972–1980.
12. Heiss P, Mayer S, Herz M, Wester HJ, Schwaiger M, Senekowitsch Schmidtke R. Investigation of transport mechanism and uptake kinetics of *O*-(2-[^{18}F]fluoroethyl)-L-tyrosine in vitro and in vivo. *J Nucl Med* 1999; 40:1367–1373.
13. Wester HJ, Herz M, Weber W, et al. Synthesis and radiopharmacology of *O*-(2-[^{18}F]fluoroethyl)-L-tyrosine for tumor imaging. *J Nucl Med* 1999; 40:205–212.
14. Babior BM. The respiratory burst of phagocytes. *J Clin Invest* 1984; 73:599–601.
15. Madri JA. Inflammation and healing. In: Kissane JM, ed. *Anderson's pathology.* St. Louis: C.V. Mosby; 1990:67–110.
16. Ritchie AC. Inflammation. In: Ritchie AC, ed. *Boyd's textbook of pathology.* Philadelphia: Lea & Febiger; 1990:60–82.
17. Sugawara Y, Gutowski TD, Fisher SJ, Brown RS, Wahl RL. Uptake of positron emission tomography tracers in experimental bacterial infections: a comparative biodistribution study of radiolabeled FDG, thymidine, L-methionine, ^{67}Ga-citrate, and ^{125}I-HSA. *Eur J Nucl Med* 1999; 26:333–341.
18. Sugawara Y, Braun DK, Kison PV, Russo JE, Zasadny KR, Wahl RL. Rapid detection of human infections with fluorine-18 fluorodeoxyglucose and positron emission tomography:

preliminary results. *Eur J Nucl Med* 1998; 25:1238–1243.
19. Stumpe KD, Dazzi H, Schaffner A, von Schulthess GK. Infection imaging using whole-body FDG-PET. *Eur J Nucl Med* 2000; 27:822–832.
20. Yamada S, Kubota K, Kubota R, Ido T, Tamahashi N. High accumulation of fluorine-18-fluorodeoxyglucose in turpentine-induced inflammatory tissue. *J Nucl Med* 1995; 36:1301–1306.
21. Kalicke T, Schmitz A, Risse JH, et al. Fluorine-18 fluorodeoxyglucose PET in infectious bone diseases: results of histologically confirmed cases. *Eur J Nucl Med* 2000; 27:524–528.
22. Jones HA, Clark RJ, Rhodes CG, Schofield JB, Krausz T, Haslett C. In vivo measurement of neutrophil activity in experimental lung inflammation. *Am J Respir Crit Care Med* 1994; 149:1635–1639.
23. Fantone JC, Ward PA. Inflammation. In: Rubin E, Farber JL, eds. *Pathology.* Philadelphia: J.B. Lippincott; 1994:33–66.
24. Senez JC. Some considerations on the energetics of bacterial growth. *Bacteriol Rev* 1962; 26:95–107.